Renewable Energy 190 (2022) 1–10

Contents lists available at ScienceDirect

Renewable Energy

journal homepage: www.elsevier.com/locate/renene

Efficient conversion of glucose into 5-HMF catalyzed by lignin-derived mesoporous carbon solid acid in a biphasic system

Shuai Wang [a, b], Thomas L. Eberhardt [c], Dayi Guo [a, b], Junfeng Feng [a, b], Hui Pan [a, b, *]

[a] Jiangsu Province Key Laboratory of Green Biomass-based Fuels and Chemicals, Nanjing, 210037, China
[b] Jiangsu Co-Innovation Center of Efficient Processing and Utilization of Forest Resources, College of Chemical Engineering, Nanjing Forestry University, Nanjing, 210037, China
[c] USDA Forest Service, Forest Products Laboratory, One Gifford Pinchot Drive, Madison, WI, 53726, USA

ARTICLE INFO

Article history:
Received 10 October 2021
Received in revised form
28 February 2022
Accepted 3 March 2022
Available online 12 March 2022

Keywords:
Lignin
Mesoporous carbon solid acid
Biphasic solvent
Glucose
5-HMF

ABSTRACT

A lignin-derived mesoporous carbon solid acid (LDMCS) catalyst was prepared by high temperature carbonization and subsequent sulfonation treatment using alkali lignin as the carbon source and KCl as a salt template. The prepared LDMCS has an irregular mesoporous structure with a narrow pore size distribution (concentrated at 4 nm), large specific surface area (1123.0 m^2 g^{-1}) and high -SO_3H group density (2.20 mmol g^{-1}). Compared with other types of solid acids reported in the literature, the prepared LDMCS catalyst has equivalent or better catalytic performance in the catalytic conversion of glucose to 5-hydroxymethylfurfural (5-HMF). A glucose conversion of 97.7% and a 5-HMF yield of 57.8% were obtained with the aqNaCl-THF (1:3) biphasic solvent system under the optimized reaction conditions with reaction temperature of 160 C, reaction time of 2.5 h, and catalyst loading of 1 mg mg^{-1}. More importantly, the 5-HMF yield still reached 40.9% after 5 cycles of the catalyst use, indicating that there was no significant loss of catalytic activity.

1. Introduction

As a value-added biomass-derived platform compound, 5-hydroxymethylfurfural (5-HMF) can be used to synthesize a variety of fuels and chemicals, such as 2,5-furanedione [1], 2,5-furandicarboxylic acid [2], 2,5-dihydroxymethylfuran [3], and 2,5-diformylfuran [4]. Renewable biomass-derived precursors such as cellulose [5], cellobiose [6], starch [7], sucrose [8], glucose [9], maltose [10], and fructose [11] have been widely studied in the production of 5-HMF. Among these 5-HMF precursors, considerable focus has been directed towards glucose because of its availability, low cost, and widespread distribution in nature as the building block for cellulose [12].

The solvent used for the catalytic conversion of glucose to 5-HMF impacts the reaction conditions needed to obtain the desired product, but also the extent that side reactions will occur. Water is undoubtedly a green and sustainable solvent, but a series of by-products can be formed in aqueous systems. Although organic solvents such as tetrahydrofuran (THF) and dimethyl sulfoxide (DMSO) as the reaction medium can give shorter reaction times and inhibit undesirable side reactions, high costs limit the application of organic solvents in the large-scale production of 5-HMF. Therefore, the catalytic conversions of glucose to 5-HMF in biphasic reaction systems with water have attracted attention. In these biphasic solvent systems, the prepared 5-HMF can be continuously extracted into the organic phase to prevent it from degrading into levulinic acid and formic acid in the aqueous phase, thereby obtaining higher glucose conversions and 5-HMF yields [13–15].

Besides the development of new solvent systems for the catalytic conversion of glucose to 5-HMF, green and effective catalysts are also of interest. To date, various homogeneous and heterogeneous acid catalysts have been developed for the conversion of glucose to 5-HMF, such as organic acids [16], mineral acids [17], ionic liquids [18], acidic resins [19], acidic zeolites [20], metal oxides [21], metal salts [22], functionalized silicas [23], coordination polymers [24], heteropolyacids [25] and carbonaceous acids [26]. Despite good catalytic efficiency under mild conditions, difficulties in separations and the corrosion of equipment are major obstacles to the commercialization of homogeneous acid catalysts [27,28]. In

* Corresponding author. Jiangsu Province Key Laboratory of Green Biomass-based Fuels and Chemicals, Nanjing, 210037, China.
E-mail address: hpan@njfu.edu.cn (H. Pan).

https://doi.org/10.1016/j.renene.2022.03.021
0960-1481/

contrast, heterogeneous (solid) acid catalysts can overcome the above-mentioned difficulties and thereby have attracted attention. Currently, porous carbon materials are widely used as catalyst supports due to their excellent chemical, physical, and thermal stability, and can be prepared from low-cost carbon resources derived from lignocellulosic biomass [29]. Lignin is a preferred precursor for the synthesis of mesoporous carbon due to its widespread availability as an industrial byproduct, but more importantly, its high carbon content. Recently, alkali metal chlorides such as ZnCl [30], LiCl [31], RbCl [32], NaCl [33], and CsCl [34] have been developed as salt templates for the synthesis of a variety of porous carbons. Compared with the widely used hard templates (such as silica) and soft templates (such as surfactants), the synthesis process of porous carbon by salt template is simpler and greener, showing broad application prospects [35,36].

In the present study, lignin-derived mesoporous carbon solid acid (LDMCS) catalysts were prepared by carbonization and sulfonation in sequence using an alkali lignin as the carbon source and KCl as the salt template. The prepared LDMCS catalysts were characterized in detail by several spectroscopies, thermal analysis, porosity determinations, scanning electron microscopy, and acid-base titration before being applied to the catalytic conversion of glucose to 5-HMF. The effects of reaction time and temperature, catalyst loading, the volume ratio of aqNaCl to THF, reaction solvent, and catalyst type on the glucose conversion and 5-HMF yield were investigated. Finally, under the optimal reaction conditions obtained, the recyclability of the LDMCS catalyst was evaluated.

2. Experimental

2.1. Materials

Alkali lignin was obtained from Sigma-Aldrich. Other common chemicals were obtained from various suppliers as follows: THF (>99.8%, Yonghua Chemical Co., Ltd.), KCl and H_2SO_4 (>99.5% and 95–98%, Nanjing Chemical Reagent Co., Ltd.), Glucose and NaCl (AR and >99.5%, Sinopharm Chemical Reagent Co., Ltd.).

2.2. Preparation of LDMCS catalysts

For the preparation of all LDMCS catalysts, alkali lignin (2.0 g) and KCl (0.5 g) were thoroughly mixed using a mortar and pestle. The mixture was transferred to a porcelain boat and carbonized in a tube furnace in two stages with a constant flow of N_2 (60 mL min ^{1}): pre-carbonization stage (ramp 30–300 C, 3 C·min ^{1}; hold at 300 C for 1 h); high-temperature carbonization stage (ramp 300–700 C, 1 C·min ^{1}; hold at 700 C for 2 h). Alkali-lignin/KCl mixtures were also carbonized at 800 and 900 C, using the same conditions (e.g., ramp rates, hold times) as before. Each carbonized product was washed with deionized water by vacuum filtration, dried at 80 C to obtain the lignin-derived porous carbon (LDMC), identified as either LDMC-700, LDMC-800 and LDMC-900 according to the carbonization temperature, and then sulfonated with concentrated sulfuric acid in a hydrothermal reactor (25 mL) at a solid-to-liquid ratio (g/mL) of 1:20, and a temperature of 180 C for 12 h. Finally, the sulfonated product was washed with deionized water by vacuum filtration until the pH of the filtrate was neutral, and then dried at 100 C to obtain the lignin-derived mesoporous carbon solid acid (LDMCS) catalyst, identified as either LDMCS-700, LDMCS-800 and LDMCS-900 (see Fig. 1 for schematic illustration of LDMCS catalyst preparation).

2.3. Characterization of LDMCS catalysts

The FT-IR spectra were collected using a Nicolet Summit infrared spectrometer in the range of 4000 to 500 cm ^{1} at a resolution of 4 cm ^{1} and 32 scans per sample. The N_2 adsorption-desorption isotherms were measured using a Micromeritics ASAP 2460 physisorption instrument using a temperature setting of 196 C; the specific surface area and pore volume were calculated by the BET method. The XRD patterns were measured with an XRD Ultima IV diffractometer using Cu Kα radiation with a scanning speed of 10 ·min ^{1} in the range of 5–80 C. The XPS spectra were measured with AXIS UltraDLD spectrometer using Al Kα radiation. Imaging by SEM used a JSM-7600F scanning electron microscope at 15 kV. Thermogravimetric analyses were carried out using a DTG-60AH thermal analyzer under N_2 atmosphere at a heating rate of 10 C·min ^{1} in the range of 30–800 C. The Raman spectra were collected with DXR532 spectrometer using 532 nm laser radiation. Finally, the -SO_3H group density (mmol·g ^{1}) was measured by WDDY-2008J microcomputer automatic potentiometric titrator according to the acid-base back titration method [37].

2.4. Catalytic conversion of glucose to 5-HMF

Catalytic conversions started with the additions of glucose (0.2 g), LDMCS (0.2 g), and aqNaCl-THF solution (1:3, by volume, 16 mL) to a high-pressure reactor (30 mL); aqNaCl refers to a saturated aqueous sodium chloride solution. Subsequently, the reactor was purged and pressurized with N_2 (1.0 MPa) to avoid side reactions of the 5-HMF generated and prevent the boiling of the reaction solution. The reaction mixture was reacted at a temperature of 160 C for 2.5 h under a stirring speed of 300 rpm. After the reaction, the high-pressure reactor was immediately quenched to room temperature. The LDMCS catalyst was separated from the reaction mixture by vacuum filtration and the filtrate set aside for analysis. The LDMCS catalyst was then washed with distilled water, dried overnight at 80 C, and used for the subsequent reactions under the same reaction conditions. After five cycles of experiments, LDMCS-700 was labeled as LDMCS-700-R. Note: In contact with air under light or anhydrous conditions, THF is very easy to generate potentially explosive peroxides. Therefore, this experiment needs to be carried out in a ventilation equipment, and standardized operations are required for subsequent product separation and analysis. In addition, protective equipment must be worn throughout the experiment.

The filtrate, containing the reaction products was membrane filtered (0.22 μm), and the contents of glucose and product were determined by HPLC (Agilent 1260 LC) equipped with a RI detector and an Aminex HPX-87H column. Sulfuric acid aqueous solution (5 mM) was used as the mobile phase at a flow rate of 0.6 mL min ^{1}, and the column and RI detector temperature were kept at 50 C. The glucose conversion, product yield and carbon balance were calculated by the following Eqs. (1)–(3), respectively:

$$Glucose\,conversion\,(\%) = 1 \frac{Moles\,of\,glucose\,unreacted}{Molesof\,glucoseadded} 100\% \quad (1)$$

$$Product\ yield\ (\%) = \frac{Moles\ of\ product\ produced}{Molesofglucoseadded} 100\% \quad (2)$$

$$Carbon\ balance\ (\%) = \frac{\sum(Moles\ of\ C\ in\ product)}{Moles\ of\ C\ in\ glucose\ converted} 100\% \quad (3)$$

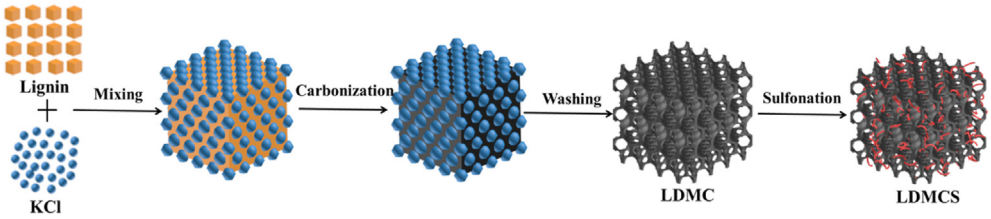

Fig. 1. Schematic illustration of synthesis of lignin-derived mesoporous carbon solid acid (LDMCS) catalyst using KCl as a salt template.

2.5. Adsorption experiments of glucose and 5-HMF

The absorption amounts of the LDMCS-700 catalyst for the glucose and 5-HMF were evaluated. Firstly, glucose (0.2 g), 5-HMF (0.08 g), LDMCS-700 (0.2 g) and aqNaCl-THF solution (1:3, by volume, 16 mL) were added to a high-pressure reactor (30 mL). Among them, the addition amount of 5-HMF selected in the adsorption experiment is the amount of 5-HMF obtained under optimized reaction conditions. Subsequently, the mixture was stirred at room temperature for 2.5 h under a stirring speed of 300 rpm. Finally, the LDMCS-700 catalyst was separated from the mixture by vacuum filtration. The filtrate, containing the glucose and 5-HMF was membrane filtered (0.22 μm), and the contents of glucose and 5-HMF were determined by HPLC mentioned above. The absorption amounts of the LDMCS-700 catalyst for the glucose and 5-HMF were calculated by the following Eq. (4):

$$Q_t = \frac{(C_0 \quad C_t) \times V}{W} \tag{4}$$

where Q_t (mg·g ^{1}) is the absorption amount of the LDMCS-700 catalyst for fructose or 5-HMF, V (mL) is the volume of solution, C_0 (mg·mL ^{1}) is the initial concentration of fructose or 5-HMF, C_t (mg·mL ^{1}) is the concentration of fructose or 5-HMF after a certain adsorption time, W (g) is the weight of LDMCS-700 catalyst.

3. Results and discussion

3.1. Structural and chemical properties of LDMCS catalysts

The LDMCS catalysts prepared at different carbonization temperatures were analyzed by FTIR spectroscopy (Fig. 2) to assess the chemical functionalities retained and those added to the alkali lignin. All three catalysts (LDMCS-700, LDMCS-800, and LDMCS-900) showed signals at 1100 cm ^{1}, 1615 cm ^{1}, and 3430 cm ^{1}, attributed to C-O, C=C, and O-H vibrations, respectively [38–40]. In addition, weak signals near 620 cm ^{1} and 1720 cm ^{1} can be attributed to the stretching vibration of C-S and the bending vibration of C=O, respectively [41]. Altogether, the FTIR results indicated that the -SO_3H group was introduced into the structure of each LDMCS catalyst by the sulfonation treatment.

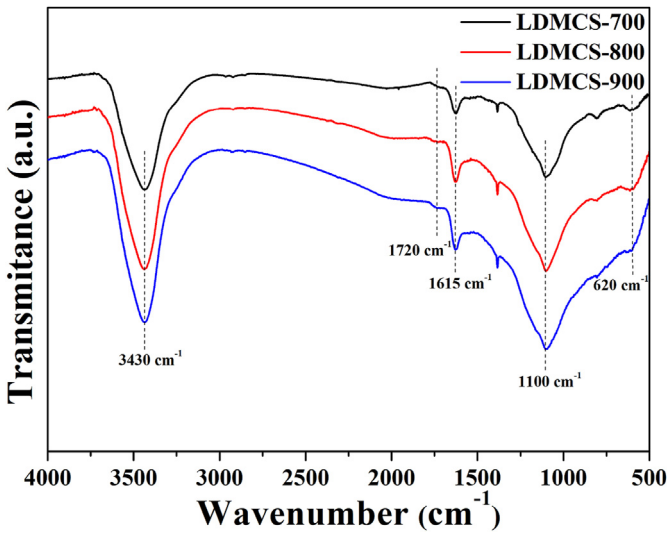

Fig. 2. FTIR spectra of LDMCS-700, LDMCS-800 and LDMCS-900 catalysts.

The XPS spectra of LDMCS catalysts prepared at different carbonization temperatures are shown in Fig. 3. All three catalysts (LDMCS-700, LDMCS-800, and LDMCS-900) exhibited three main signals in the full spectra (Fig. 3a,d,g) at 168.6, 284 and 531 eV, which are assigned to S 2p, C 1s and O 1s, respectively [38]. The C 1s spectra (Fig. 3b,e,h) could each be fitted with four component peaks at 284.6, 284.9, 286.0 and 289.0 eV, corresponding to C-S, C=C, C-O and C=O, respectively [42,43]. The O 1s spectra (Fig. 3c,f,i) was only fitted with two component peaks at 532.0 and 533.4 eV, which are assigned to C=O and C-O, respectively [44]. The S 2p spectra (see inset of Fig. 3a,d,g) exhibited a single peak each at 168.4 eV corresponding to the -SO_3H group [45]. These results further confirmed that the -SO_3H group was introduced into the structure of each LDMCS catalyst by the sulfonation treatment.

The XRD patterns and Raman spectra of LDMCS catalysts are shown in Fig. 4a and Fig. 4b, respectively. The XRD patterns (Fig. 4a) show that all the LDMCS catalysts prepared at the three different carbonization temperatures exhibited a broad peak at 23 and a weak peak at 44 , which correspond to (002) and (100) diffraction planes, respectively, consistent a partially graphitized structure [46]. Likewise, the Raman spectra (Fig. 4b) gave results consistent with a partially graphitized structure. Specifically, all the LDMCS catalysts exhibited two peaks; the peak at 1340 cm ^{1} (D-band), and the peak at 1590 cm ^{1} (G-band), correspond to the defects within the carbon micro-textures and a well-defined graphitized structure [47], respectively.

The N_2 adsorption-desorption isotherms and pore size distribution curves of the catalysts are shown in Fig. 5. All three adsorption-desorption isotherms (Fig. 5a) have a typical IV-type curve with an obvious H4 hysteresis loop. The sharp increase in N_2 adsorption at low relative pressure, and the presence of H4-type hysteresis loop at medium relative pressure, together indicate the co-existence of both microporous and mesoporous structures. The pore-size distributions (Fig. 5b) of all three catalysts were mainly concentrated around 4.0 nm.

The results in Table 1 show that the carbonization temperature had an influence on the structural characteristics of the LDMCS catalysts. For LDMCS-700, the pore volume (V_{total}) was higher (0.61 cm^3 g ^{1}) and average pore diameter (D) was smaller (3.6 nm) than for the other two LDMCS catalysts (V_{total} = 0.49 cm^3 g ^{1}; D = 4.5 nm). With the increase of carbonization temperature, the specific surface area (S_{BET}) trended downward; this is attributed to the collapse of the pore structure caused by high-temperature

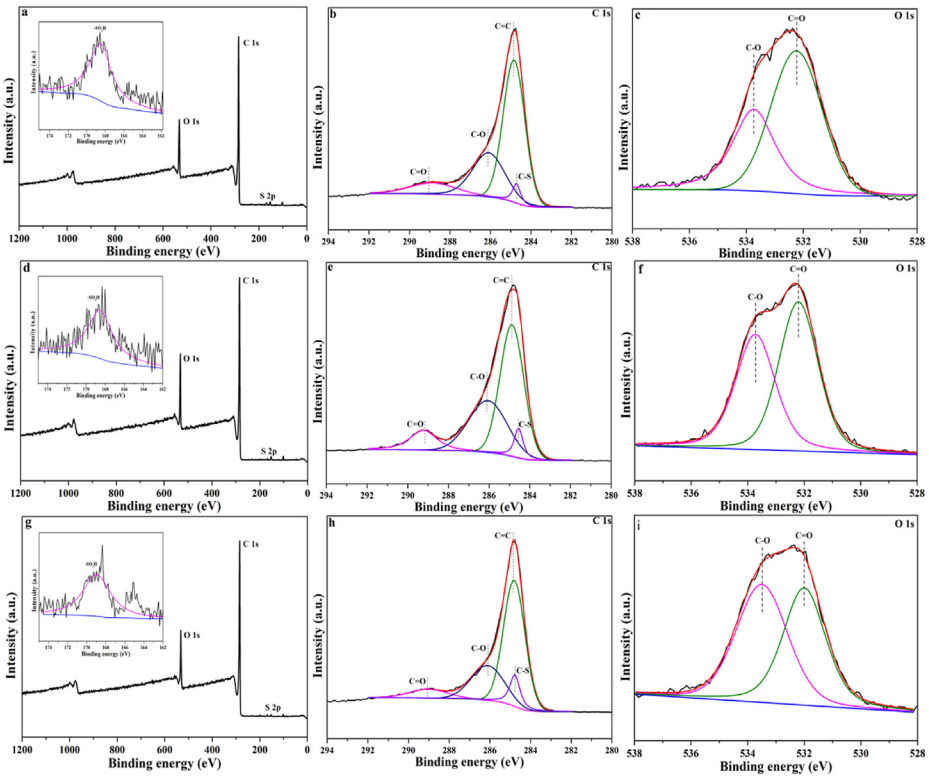

Fig. 3. XPS spectra of LDMCS-700 (a, b and c), LDMCS-800 (d, e and f) and LDMCS-900 (g, h and i) catalysts.

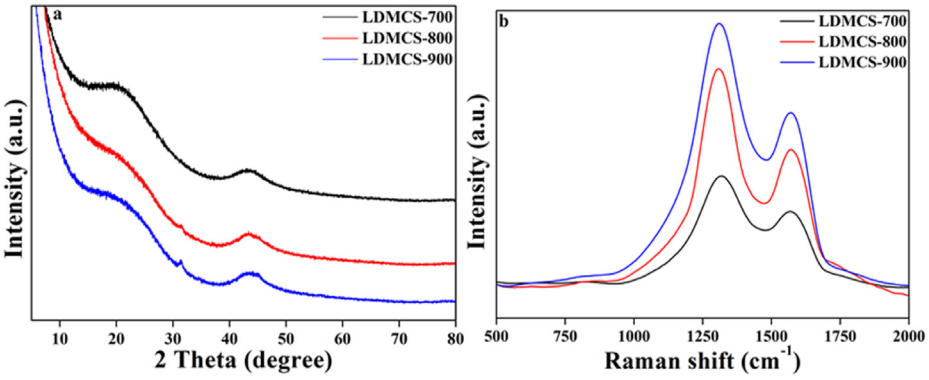

Fig. 4. XRD patterns (a) and Raman spectra (b) of LDMCS-700, LDMCS-800 and LDMCS-900 catalysts.

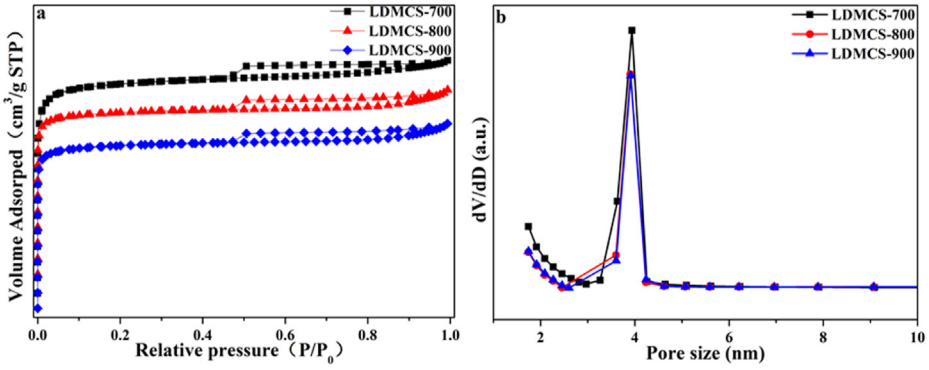

Fig. 5. N_2 adsorption-desorption isotherms (a) and pore size distribution (b) of LDMCS-700, LDMCS-800 and LDMCS-900 catalysts.

Table 1
Structural parameters of LDMCS-700, LDMCS-800 and LDMCS-900 catalysts.

Catalyst	S_{BET} ($m^2 \cdot g^{-1}$)	V_{total} ($cm^3 \cdot g^{-1}$)	D (nm)
LDMCS-700	1123.0	0.61	3.6
LDMCS-800	956.6	0.49	4.5
LDMCS-900	887.6	0.49	4.5

carbonization.

The surface morphology of LDMCS catalysts prepared under different carbonization temperatures are shown in Fig. 6. As seen from SEM images, all the LDMCS catalysts exhibited irregular and porous surface structures with micron-scale pores, indicating they also contained a certain amount of macropores. In addition, the appearance of fine particles and faults may be caused by subsequent sulfonation [48–50].

The thermal stability of the three LDMCS catalysts was demonstrated by TGA, and as expected, the LDMCS-700 catalyst was the least stable (Fig. 7). As seen from Fig. 7a, all LDMCS catalysts showed weight loss near 100 C from the evaporation of water. The most significant weight loss near 220 C is likely from the conversion of -SO_3H groups into volatile sulfide molecules [51]. Given that the largest weight loss rate (Fig. 7b) was near 220 C, the range of reaction temperatures for the glucose conversions was set between 140 C and 190 C to ensure the thermal stability of LDMCS catalyst.

3.2. Catalytic performance of LDMCS catalysts

3.2.1. Effect of carbonization temperature

The catalytic performance of LDMCS catalysts prepared at different carbonization temperatures for the conversion of glucose to 5-HMF was studied using a reaction temperature of 160 C, reaction time of 3 h, catalyst loading of 1 mg mg ^{1}, and an aqNaCl to THF volume ratio of 1:3 (Table 2). Results show that the 5-HMF yield is significantly affected by the carbonization temperature, with LDMCS-700 resulting in the highest yield of 55.1% and LDMCS-900 having the lowest yield of 44.6%. The higher catalytic activity of LDMCS-700, compared to both LDMCS-800 and LDMCS-900 is attributed to its higher specific surface area (Table 1) and -SO_3H group density (Table 2), the former being conducive to the diffusion of glucose into the particle pores and the latter providing more active sites for catalysis.

In addition, the catalytic effects of catalysts LDMCS-700 and LDMCS-900 were compared based on the same amount of -SO_3H group, and the results are shown in Table S1. It was found that when the amounts of -SO_3H groups of these two catalyst were similar, in other words, the amount of LDMCS-900 was double of LDMCS-700, they demonstrated similar catalytic activities on the conversion of glucose to 5-HMF, indicating that the amount of -SO_3H group is the key factor determining the catalytic activity.

3.2.2. Effects of reaction time and temperature

The effects of reaction time and temperature were determined for the best performing catalyst (see Table 2), that being LDMCS-700. When the reaction time was 1.5 h, the glucose conversion and 5-HMF yield were 59.1% and 26.8%, respectively (Fig. 8a), with constant conditions for reaction temperature (160 C), catalyst loading (1 mg mg ^{1}) and aqNaCl to THF volume ratio (1:3). As the reaction time increased to 2.5 h, the glucose conversion and 5-HMF yield increased to 97.7% and 57.8%, respectively. With the further increase of the reaction time (3.0 h), the yield of 5-HMF decreased slightly, likely from the occurrence of undesirable side reactions, such as rehydrations of 5-HMF to levulinic acid and/or formic acid.

The results from varying the reaction temperature, with a constant condition for reaction time (2.5 h), catalyst loading (1 mg mg ^{1}), and aqNaCl to THF volume ratio (1:3), are shown in Fig. 8b. When the reaction temperature was 140 C, the glucose conversion and 5-HMF yield were each very low, at 29.1% and 5.4%, respectively. When the reaction temperature increased to 160 C, the glucose conversion and 5-HMF yield increased significantly to 97.7% and 57.8%, respectively. Upon further increases in the reaction temperature, there was a stepwise decrease in the yield of 5-HMF. These reductions in 5-HMF yield are attributed to the higher temperatures causing undesirable side reactions, such as the polymerization of 5-HMF into humins. Based on the above results, the optimal reaction time and temperature for the catalytic conversion of glucose to 5-HMF via the LDMCS-700 catalyst are 2.5 h and 160 C, respectively.

3.2.3. Effect of catalyst loading

The effect of LDMCS-700 catalyst loading on glucose conversion and 5-HMF yield was then investigated for the LDMCS-700 catalyst, and the results are shown in Fig. 9; here the reaction conditions for reaction time (2.5 h), reaction temperature (160 C) and aqNaCl to THF volume ratio (1:3) were held constant. As shown in Fig. 9, the catalyst loading has a significant impact on the conversion of glucose and the production of 5-HMF. When no catalyst was added to the reaction system, the conditions were sufficiently acidic to convert 51.9% of the glucose; the yield of 5-HMF yield was 25.3%. When the catalyst was added, using a small loading of 0.25 mg mg ^{1}, the glucose conversion and 5-HMF yield were improved to 76.5% and 40.1%, respectively. With further increases in catalyst loading, the glucose conversion and 5-HMF yield increased stepwise, reaching the maximum values (97.7% and 57.8%, respectively) at the catalyst loading of 1 mg mg ^{1}. With further increases in the catalyst loading, the glucose conversion showed little change, but there was a small decrease in 5-HMF yield. Thus, an excess

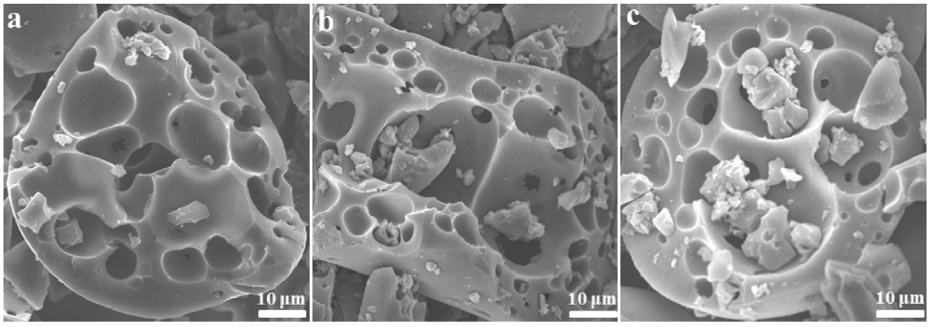

Fig. 6. SEM images of LDMCS-700 (a), LDMCS-800 (b) and LDMCS-900 (c) catalysts.

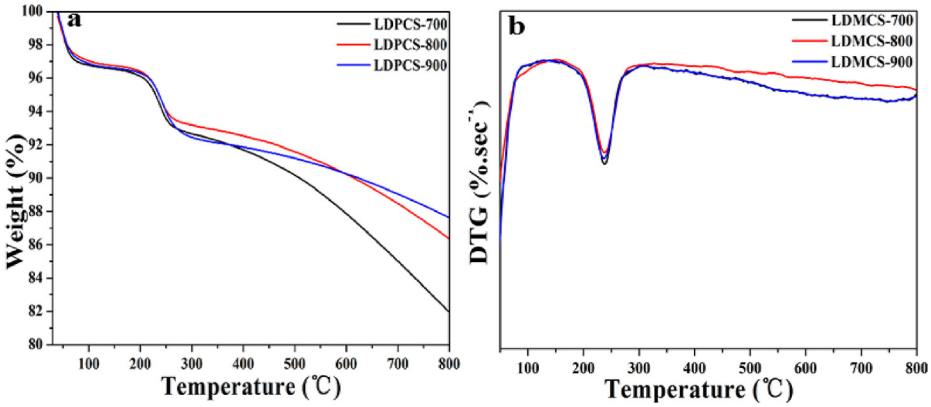

Fig. 7. TGA (a) and DTG (b) curves of LDMCS-700, LDMCS-800 and LDMCS-900 catalysts.

Table 2
The effect of carbonization temperature on glucose conversion and 5-HMF yield.

Catalyst	Glucose conversion (%)	5-HMF yield (%)	-SO_3H density (mmol·g ^{1})
LDMCS-700	99.3	55.1	2.20
LDMCS-800	98.8	49.2	1.40
LDMCS-900	98.9	44.6	1.12

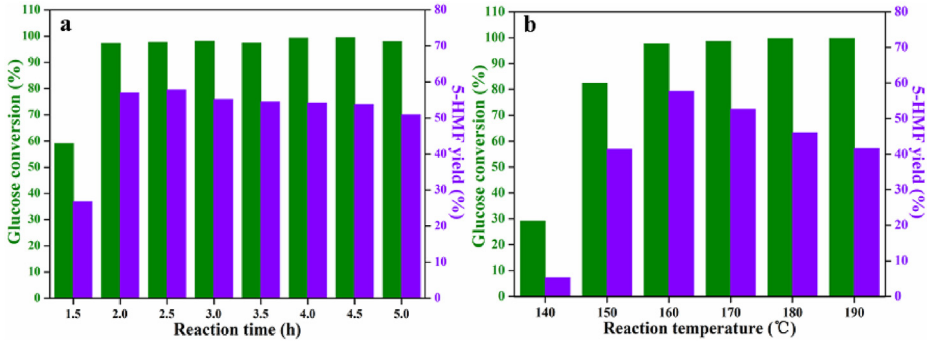

Fig. 8. The effects of reaction time (a) and temperature (b) on the catalytic conversion of glucose to 5-HMF. Reaction conditions: (a) reaction temperature of 160 C, LCMCS-700 catalyst loading of 1 mg mg ^{1}, and aqNaCl to THF volume ratio of 1:3; (b) reaction time of 2.5 h, LCMCS-700 catalyst loading of 1 mg mg ^{1}, and aqNaCl to THF volume ratio of 1:3.

catalytic active sites in the reaction system would seem to promote side reactions such as the rehydration of 5-HMF to levulinic acid, formic acid, and/or the polymerization of 5-HMF into humins [52]. Alternatively, excessive solid acid added to the biphasic solvent system could have been suspended between the water phase and the organic phase, thereby affecting the extraction of organic phase to recover the 5-HMF.

3.2.4. Effect of volume ratio of aqNaCl to THF

Generally, the addition of an appropriate amount of organic solvent (such as THF) to the aqueous phase reaction system helps to inhibit the occurrence of 5-HMF side reactions, thereby improving yields; the prepared 5-HMF can be continuously extracted into the organic phase through the phase separation afforded by the aqNaCl-THF mixed solvent system (see Fig. 10a). Additionally, the use of a mixed solvent system, with aqueous and organic phases, can also reduce the use of organic solvents, thereby providing possible opportunities to reduce production costs and environmental pollution. The effect of the volume ratio of aqNaCl to THF on the glucose conversion and 5-HMF yield was explored, and the results are shown in Fig. 10b. A low glucose conversion of 68.3% and very low 5-HMF yield of 12.5% were obtained in using the pure NaCl saturated aqueous solution alone. With the addition of THF to the reaction system, the glucose conversion and 5-HMF yield both increased significantly, and reached the maximum values (97.7% and 57.8%, respectively) using an aqNaCl to THF volume ratio of 1:3. The advantage of the biphasic solvent system used in the present study is clearly demonstrated by a very low yield of 5-HMF (2.8%) in THF alone, despite a high conversion of glucose (96.5%).

3.2.5. Effects of reaction solvent and catalyst type

The effects of reaction solvent and catalyst type on the catalytic conversion of glucose to 5-HMF are shown in Fig. 11a and Fig. 11b, respectively. As shown in Fig. 11a, the catalytic performance of LDMCS-700 in a single phase system of H_2O, THF, DMSO, and N,N-Dimethylformamide (DMF) were all much lower than that of the aqNaCl-THF biphasic solvent system; although the organic solvents alone gave comparable conversions of glucose, the 5-HMF yields were all very low (<12.9%). With the aqNaCl-THF biphasic solvent system as the reaction medium, the 5-HMF that was generated could be continuously extracted into the organic phase, thereby reducing its conversion into levulinic acid and formic acid by rehydration.

Results presented up to this point demonstrate that lignin-

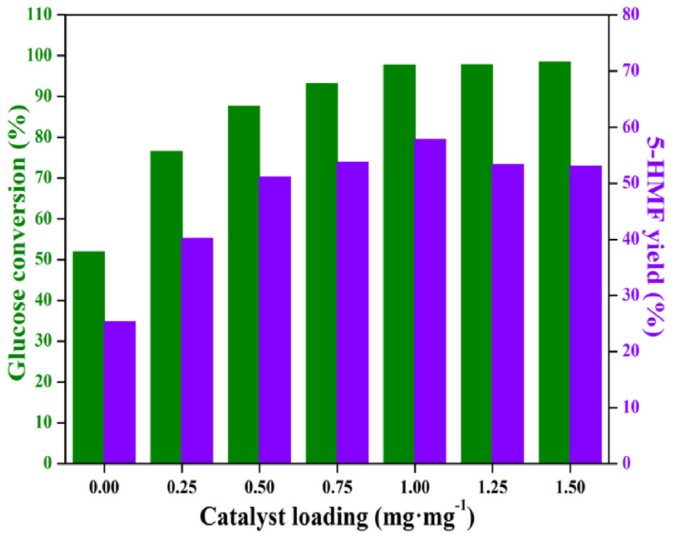

Fig. 9. The effect of LDMCS-700 catalyst loading on the catalytic conversion of glucose to 5-HMF. Reaction conditions: reaction time of 2.5 h, and reaction temperature of 160 C, and aqNaCl to THF volume ratio of 1:3.

derived catalysts developed in the current study were clearly useful for the conversion of glucose to 5-HMF, particularly when using the aqNaCl-THF biphasic solvent system. For comparison to currently available commercial catalysts such as metal oxides (Nb_2O_5), heteropolyacids (phosphotungstic acid, PTA), metal chlorides ($FeCl_3$), molecular sieves (HZSM-5), and acid ion exchange resin (Amberlyst-15), these alternative catalysts were used in reactions carried out using the optimum reaction conditions for LDMCS-700. Although this comparison is does not optimize the reaction conditions for these other catalysts, Fig. 11b shows in relative terms that LDMCS-700 performs well, and we can attribute this to its high specific surface area and -SO_3H group density. In addition, it was found that the adsorption amounts of LDMCS-700 catalyst for glucose and 5-HMF were 195.2 mg g ^{1} and 45.4 mg g ^{1}, respectively. The adsorption amount of LDMCS-700 catalyst for glucose is higher than that of 5-HMF, which helps the conversion of glucose and reduces the occurrence of side reactions related to 5-HMF. This may be another reason why the LDMCS-700 catalyst has outstanding catalytic performance in the conversion of glucose to 5-HMF.

And the catalytic performance of LDMCS-700 also compares well to different sulfonated solid acids in different reaction solvents reported in the literature for the catalytic conversion of glucose to 5-HMF (Table 3). Overall, in the present study we demonstrate the lignin-derived mesoporous carbon solid acid can be prepared that has better catalytic performance than many other solid acid catalytic systems.

3.2.6. *Stability of LDMCS catalysts*

In order to investigate the stability of LDMCS catalysts for the conversion of glucose to 5-HMF with the aqNaCl-THF biphasic

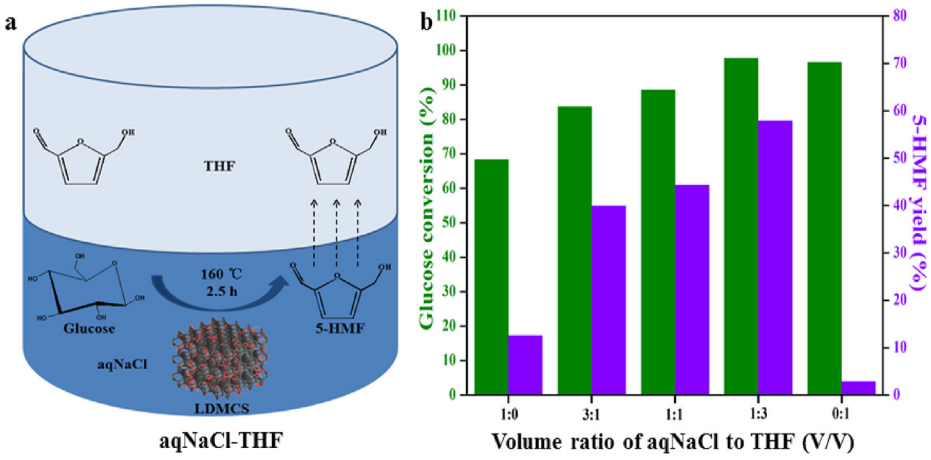

Fig. 10. (a) Schematic illustration of the LDMCS-700 catalytic conversion of glucose to 5-HMF and (b) The effect of volume ratio of aqNaCl to THF on the catalytic conversion of glucose to 5-HMF. Reaction conditions: reaction time of 2.5 h, reaction temperature of 160 C, and catalyst loading of 1 mg mg ^{1}.

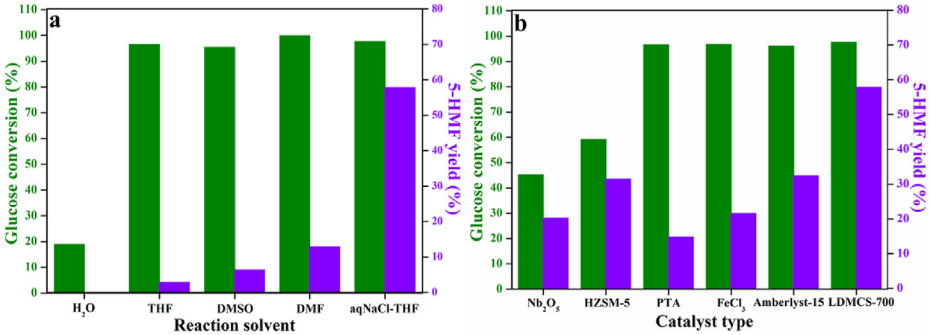

Fig. 11. The effects of reaction solvent (a) and catalyst type (b) on the catalytic conversion of glucose to 5-HMF. Reaction conditions: reaction time of 2.5 h, reaction temperature of 160 C, catalyst loading of 1 mg mg ^{1}, and aqNaCl to THF volume ratio of 1:3.

Table 3
Catalytic performance of different sulfonated solid acids for the conversion of glucose to 5-HMF in different solvents.

Catalyst	Solvent	Time (h)	Temp (C)	Glucose Conversion (%)	5-HMF Yield (%)
MPR-SO_3H/Yb(OTf)$_2$ [53]	SBP/H_2O	4	170	75.0	52.0
MCM-41-IM-HSO_4-Cr(III) [54]	DMSO	4	140	99.0	43.5
MIL-101(Cr)-SO_3H [55]	THF/H_2O	24	130	–	34.0
MIL-101(Cr)-SO_3H [56]	GVL/H_2O	2	150	–	44.9
UIO-66(Zr)SO_3H/PDA-PU [57]	DMSO	2	120	–	56.6
UiO-66(Zr)-SO_3H-NH_2/PDA-GO [58]	DMSO	2	120	–	55.8
UIO-66(Zr)-SO_3H-NH_2 [59]	DMSO	12	140	–	49.7
PCP(Sn)-SO_3H/PDA-MnO_2 [60]	THF/H_2O	6	150	73.2	41.2
PCP(Sn)-SO_3H-IMD [61]	THF/H_2O	5	160	–	49.8
MAM-CNC-COF-SO_3H/SBA-15 [24]	DMSO	4	120	70.0	45.0
CNT-SO_3H [62]	DMSO	1	140	99.0	57.0
CNF-SO_3H [62]	DMSO	1	140	99.0	46.0
pTSA-Ca/AC [63]	MIBK/H_2O	24	180	91.0	57
β-cyclodextrin-SO_3H [64]	DMSO	5	180	–	47.0
AC-Zn-SO_3H [65]	aqNaCl-THF	8	160	65.4	51.0
LDMCS-700 (This work)	aqNaCl-THF	2.5	160	97.7	57.8

Note: SBP, GVL and MIBK are 2-sec-butylphenol, γ-valerolactone and methyl isobutyl ketone, respectively.

solvent system, five reaction cycles were carried out, repeatedly using same sample of LDMCS-700. As shown in Fig. 12, there was a small stepwise reduction in 5-HMF yield; however, the 5-HMF yield remained reasonably high at 40.2% after five cycles. In addition, the weight loss of LDMCS-700 after each cycle under optimized conditions was recorded and shown in Table S2. To further explore the changes of the LDMCS-700 catalyst after five cycles of experiments, recovered catalyst LDMCS-700-R was characterized. Compared with LDMCS-700 (2.20 mmol g ^{1}), it was found that the -SO_3H group density of LDMCS-700-R decreased to 1.20 mmol g ^{1} after five reaction cycles, which in turn caused the decrease of 5-HMF yield. The N_2 adsorption-desorption isotherm and pore size distribution curve of LDMCS-700-R (Fig. S1) suggest that the catalyst still maintained its original carbon skeleton structure. In addition, as listed in Table S3, the specific surface area and pore volume of LDMCS-700-R decreased from 1123.0 m^2 g ^{1} and 0.61 cm^3 g ^{1} to 919.4 m^2 g ^{1} and 0.45 cm^3 g ^{1}, respectively, which should be attributed to the blocking of some pore structure by reaction byproducts such as humins. The decrease of specific area would cause less efficient absorption of reaction substrate and consequently resulted in decreased product yield. Based on the above results, it could be concluded that the decrease in the catalytic activity of the LDMCS-700 catalyst after five reaction cycles was due to the changes to the catalyst itself, such as the loss of -SO_3H groups on its structure as well as partially blocking of its porous structure during the conversion process [66].

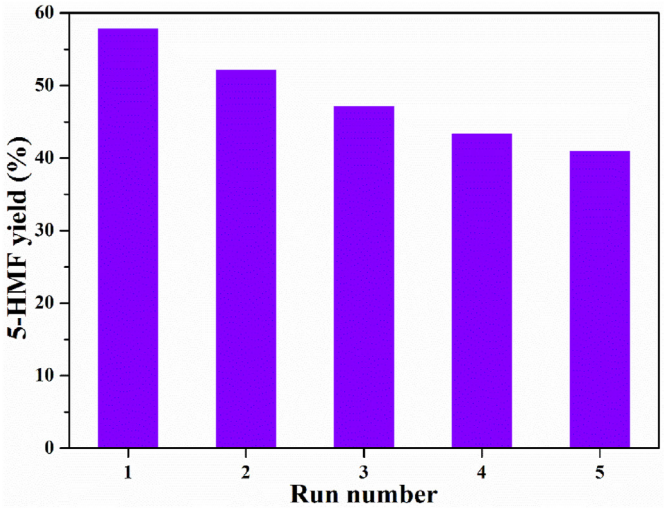

Fig. 12. Catalyst reusability in the catalytic conversion of glucose to 5-HMF. Reaction condition: Reaction time of 2.5 h, reaction temperature 160 C, catalyst loading of 1 mg mg ^{1} and aqNaCl to THF volume ratio of 1:3.

3.2.7. Assessment of carbon balance and the amount of waste liquid generated

The main product yields and carbon balance in the catalytic conversion of glucose to 5-HMF with LDMCS-700 under optimized conditions are shown in Table S4. It can be seen that the glucose conversion was 97.7%, and the total yield of these 4 main products was around 80.0%. In addition, after calculation, the carbon balance here was 65.7%. Other reaction products were not detected by high performance liquid chromatography, which should be oligomers and humins that are commonly generated during reactions involved carbohydrate [67]. In addition, the amount of waste liquid generated from the conversion of glucose to 5-HMF catalyzed by lignin-derived mesoporous carbon solid acid was also calculated based on per kg of 5-HMF production (no consideration of catalyst reusability). There are mainly three generation stages of waste liquid. Firstly, the preparation of the lignin-derived porous carbon-based support involves the removal of KCl by water washing, approximately 300 mL of waste liquid was generated. Secondly, the sulfonation of the lignin-derived porous carbon-based support involves the removal of the free H_2SO_4 by water washing, approximately 2500 mL of waste liquid was generated. Finally, the catalytic conversion of glucose to 5-HMF involves the addition of an aqNaCl-THF biphasic reaction solvent, approximately 200 mL of waste liquid was generated. Based on the above results, it is found that around 3 kg of waste liquid was generated based on per kg of 5-HMF production.

4. Conclusions

A series of LDMCS catalysts were prepared by carbonization and sulfonation of an alkali lignin, a biomass-based carbon source with inherently high carbon content; this was done using KCl as a salt template. Compared with sulfonated solid acids and other types of solid acids, the prepared LDMCS can achieve effective catalytic conversion of glucose to 5-HMF in an aqNaCl-THF biphasic solvent system under relatively mild reaction conditions. Using a reaction temperature of 160 C, reaction time of 2.5 h, and catalyst loading of 1 mg mg ^{1}, a glucose conversion of 97.7% and 5-HMF yield of 57.8% were achieved. Thus, these lignin-derived solid acid catalysts had sufficient catalytic active sites available, and these are attributed to

their high specific surface area and -SO_3H group density. Finally, using the aqNaCl-THF biphasic solvent system as the reaction medium, the 5-HMF generated could be continuously extracted into the organic phase, thereby inhibiting undesirable side reactions that can reduce the 5-HMF yield.

CRediT authorship contribution statement

Shuai Wang: Investigation, Writing – original draft. **Thomas L. Eberhardt:** Writing – review & editing, Supervision. **Dayi Guo:** Writing – review & editing. **Junfeng Feng:** Writing – review & editing. **Hui Pan:** Conceptualization, Writing – review & editing.

Declaration of competing interest

The authors declare that they have no known competing financial interests or personal relationships that could have appeared to influence the work reported in this paper.

Acknowledgements

The authors are grateful for the financial support from National Natural Science Foundation of China (No.31770631) and National Key Basic Research Program of China (2017YFD0601005).

Appendix A. Supplementary data

Supplementary data to this article can be found online at https://doi.org/10.1016/j.renene.2022.03.021.

References

[1] Y. Rodenas, R. Mariscal, J.L.G. Fierro, D.M. Alonso, J.A. Dumesic, M.L. Granados, Improving the production of maleic acid from biomass: TS-1 catalysed aqueous phase oxidation of furfural in the presence of gamma-valerolactone, Green Chem 20 (2018) 2845–2856.
[2] E. Hayashi, Y. Yamaguchi, K. Kamata, N. Tsunoda, Y. Kumagai, F. Oba, M. Hara, Effect of MnO_2 crystal structure on aerobic oxidation of 5-hydroxymethylfurfural to 2,5-furandicarboxylic acid, J. Am. Chem. Soc. 141 (2019) 890–900.
[3] L. Hu, N. Li, X. Dai, Y. Guo, Y. Jiang, A. He, J. Xu, Highly efficient production of 2,5-dihydroxymethylfuran from biomass-derived 5-hydroxymethylfurfural over an amorphous and mesoporous zirconium phosphonate catalyst, J. Energy Chem. 37 (2019) 82–92.
[4] J.L. DiMeglio, A.G. Breuhaus-Alvarez, S. Li, B.M. Bartlett, Nitrate-mediated alcohol oxidation on cadmium sulfide photocatalysts, ACS Catal 9 (2019) 5732–5741.
[5] J. Wan, J. Lian, Y. Wang, Y. Ma, Investigation of cellulose supramolecular structure changes during conversion of waste paper in near-critical water on producing 5-hydroxymethyl furfural, Renew. Energy 80 (2015) 132–139.
[6] M. Li, X. Yu, C. Zhou, A.E.A. Yagoub, Q. Ji, L. Chen, Construction of an integrated platform for 5-HMF production and separation based on ionic liquid aqueous two-phase system, J. Mol. Liq. 313 (2020), 113529.
[7] F. Yang, J. Weng, J. Ding, Z. Zhao, L. Qin, F. Xia, Effective conversion of saccharides into hydroxymethylfurfural catalyzed by a natural clay, attapulgite, Renew. Energy 151 (2020) 829–836.
[8] S. Yu, H. Zang, X. Yang, M. Zhang, R. Xie, P. Yu, Highly efficient preparation of 5-hydroxymethylfurfural from sucrose using ionic liquids and heteropolyacid catalysts in dimethyl sulfoxide–water mixed solvent, Chin. Chem. Lett. 28 (2017) 1479–1484.
[9] R. Goyal, B.M. Abraham, O. Singh, S. Sameer, R. Bal, P. Mondal, One-pot transformation of glucose into hydroxymethyl furfural in water over Pd decorated acidic ZrO_2, Renew. Energy 183 (2022) 791–801.
[10] G. Qiu, B. Chen, C. Huang, N. Liu, X. Sun, Tin-modified ionic liquid polymer: a novel and efficient catalyst for synthesis of 5-hydroxymethylfurfural from glucose, Fuel 268 (2020), 117136.
[11] S. Karimi, F. Seidi, M. Niakan, H. Shekaari, M. Masteri-Farahani, Catalytic dehydration of fructose into 5-hydroxymethylfurfural by propyl sulfonic acid functionalized magnetic graphene oxide nanocomposite, Renew. Energy 180 (2021) 132–139.
[12] M. Li, W. Li, Y. Lu, H. Jameel, H. Chang, L. Ma, High conversion of glucose to 5-hydroxymethylfurfural using hydrochloric acid as a catalyst and sodium chloride as a promoter in a water/γ-valerolactone system, RSC Adv 7 (2017) 14330–14336.
[13] E. Combs, B. Cinlar, Y. Pagan-Torres, J.A. Dumesic, B.H. Shanks, Influence of alkali and alkaline earth metal salts on glucose conversion to 5-hydroxymethylfurfural in an aqueous system, Catal. Commun. 30 (2013) 1–4.
[14] Y. Román-Leshkov, C.J. Barrett, Z.Y. Liu, J.A. Dumesic, Production of dimethylfuran for liquid fuels from biomass-derived carbohydrates, Nature 447 (2007) 982–985.
[15] Y. Román-Leshkov, J.A. Dumesic, Solvent effects on fructose dehydration to 5-hydroxymethylfurfural in biphasic systems saturated with inorganic salts, Top. Catal. 52 (2009) 297–303.
[16] H.M. Mirzaei, B. Karimi, Sulphanilic acid as a recyclable bifunctional organocatalyst in the selective conversion of lignocellulosic biomass to 5-HMF, Green Chem 18 (2016) 2282–2286.
[17] J.N. Chheda, Y. Román-Leshkov, J.A. Dumesic, Production of 5-hydroxymethylfurfural and furfural by dehydration of biomass-derived mono-and poly-saccharides, Green Chem 9 (2007) 342–350.
[18] Z. Hu, B. Liu, Z. Zhang, L. Chen, Conversion of carbohydrates into 5-hydroxymethylfurfural catalyzed by acidic ionic liquids in dimethyl sulfoxide, Ind. Crop. Prod. 50 (2013) 264–269.
[19] G. Morales, J.A. Melero, M. Paniagua, J. Iglesias, B. Hernández, M. Sanz, Sulfonic acid heterogeneous catalysts for dehydration of C6-monosaccharides to 5-hydroxymethylfurfural in dimethyl sulfoxide, Chin. J. Catal. 35 (2014) 644–655.
[20] L. Hu, Z. Wu, J. Xu, Y. Sun, L. Lin, S. Liu, Zeolite-promoted transformation of glucose into 5-hydroxymethylfurfural in ionic liquid, Chem. Eng. J. 244 (2014) 137–144.
[21] Q. Hou, M. Zhen, W. Li, L. Liu, J. Liu, S. Zhang, Y. Nie, C. Bai, X. Bai, M. Ju, Efficient catalytic conversion of glucose into 5-hydroxymethylfurfural by aluminum oxide in ionic liquid, Appl. Catal. B Environ. 253 (2019) 1–10.
[22] M. Ohara, A. Takagaki, S. Nishimura, K. Ebitani, Syntheses of 5-hydroxymethylfurfural and levoglucosan by selective dehydration of glucose using solid acid and base catalysts, Appl. Catal. A-Gen. 383 (2010) 149–155.
[23] M. Walia, U. Sharma, V.K. Agnihotri, B. Singh, Silica-supported boric acid assisted conversion of mono-and poly-saccharides to 5-hydroxymethylfurfural in ionic liquid, RSC Adv 4 (2014) 14414–14418.
[24] Z. Babaei, A.N. Chermahini, M. Dinari, M. Saraji, A. Shahvar, A sulfonated triazine-based covalent organic polymer supported on a mesoporous material: a new and robust material for the production of 5-hydroxymethylfurfural, Sustain. Energy Fuels 3 (2019) 1024–1032.
[25] P. Zhao, Y. Zhang, Y. Wang, H. Cui, F. Song, X. Sun, L. Zhang, Conversion of glucose into 5-hydroxymethylfurfural catalyzed by acid-base bifunctional heteropolyacid-based ionic hybrids, Green Chem 20 (2018) 1551–1559.
[26] L. Hu, G. Zhao, X. Tang, Z. Wu, J. Xu, L. Lin, S. Liu, Catalytic conversion of carbohydrates into 5-hydroxymethylfurfural over cellulose-derived carbonaceous catalyst in ionic liquid, Bioresour. Technol. 148 (2013) 501–507.
[27] B. Liu, Z. Zhang, One-pot conversion of carbohydrates into furan derivatives via furfural and 5-hydroxylmethylfurfural as intermediates, ChemSusChem 9 (2016) 2015–2036.
[28] M. Lopes, K. Dussan, J.J. Leahy, V.T. da Silva, Conversion of ID-glucose to 5-hydroxymethylfurfural using Al_2O_3-promoted sulphated tin oxide as catalyst, Catal. Today 279 (2017) 233–243.
[29] Z. Ma, H. Zhang, Z. Yang, Y. Zhang, B. Yu, Z. Liu, Highly mesoporous carbons derived from biomass feedstocks templated with eutectic salt $ZnCl_2$/KCl, J. Mater. Chem. 2 (2014) 19324–19329.
[30] S. Gao, X. Li, L. Li, X. Wei, A versatile biomass derived carbon material for oxygen reduction reaction, supercapacitors and oil/water separation, Nano Energy 33 (2017) 334–342.
[31] H.K. Kim, A.R. Kamali, K.C. Roh, K.B. Kim, D.J. Fray, Dual coexisting interconnected graphene nanostructures for high performance supercapacitor applications, Energy Environ. Sci. 9 (2016) 2249–2256.
[32] A. Platek-Mielczarek, C. Nita, C.M. Ghimbeu, E. Frackowiak, K. Fic, Link between alkali metals in salt templates and in electrolytes for improved carbon-based electrochemical capacitors, ACS Appl. Mater. Interfaces 13 (2021) 2584–2599.
[33] B. Liu, M. Yang, H. Chen, Y. Liu, D. Yang, H. Li, Graphene-like porous carbon nanosheets derived from salvia splendens for high-rate performance supercapacitors, J. Power Sources 397 (2018) 1–10.
[34] T. Yan, Z. Wan, K. Wang, M. Hu, X. Wang, A 3D carbon foam derived from phenol resin via CsCl soft-templating approach for high-performance supercapacitor, Energy Technol 8 (2020), 1901301.
[35] D. Qiu, T. Cao, J. Zhang, S. Zhang, D. Zheng, H. Wu, W. Lv, F. Kang, Q. Yang, Precise carbon structure control by salt template for high performance sodium-ion storage, J. Energy Chem. 31 (2019) 101–106.
[36] A. Lu, W. Li, W. Schmidt, F. Schuth, Fabrication of hierarchically structured carbon monoliths via self-binding and salt templating, Microporous Mesoporous Mater. 95 (2006) 187–192.
[37] S. Wang, G. Sima, Y. Cui, L. Chang, L. Gan, Efficient hydrolysis of cellulose to glucose catalyzed by lignin-derived mesoporous carbon solid acid in water, Chin. J. Chem. Eng. 28 (2020) 1866–1874.
[38] W. Song, Y. Zhang, A. Varyambath, J.S. Kim, I. Kim, Sulfonic acid modified hollow polymer nanospheres with tunable wall-thickness for improving biodiesel synthesis efficiency, Green Chem 22 (2020) 3572–3583.
[39] S. Shen, B. Cai, C. Wang, H. Li, G. Dai, H. Qin, Preparation of a novel carbon-based solid acid from cocarbonized starch and polyvinyl chloride for cellulose hydrolysis, Appl. Catal. A-Gen. 473 (2014) 70–74.
[40] S.H. Shim, K.T. Kim, J.U. Lee, W.H. Jo, Facile method to functionalize graphene

oxide and its application to poly(ethylene terephthalate)/graphene composite, ACS Appl. Mater. Interfaces 4 (2012) 4184–4191.
[41] H. Li, X. Zhang, Q. Wang, D. Yang, Q. Cao, L. Jin, Study on the hydrolysis of cellulose with the regenerable and recyclable multifunctional solid acid as a catalyst and its catalytic hydrolytic kinetics, Cellulose 27 (2020) 285–300.
[42] K. Dong, J. Zhang, W. Luo, L. Su, Z. Huang, Catalytic conversion of carbohydrates into 5-hydroxymethyl furfural over sulfonated hyper-cross-linked polymer in DMSO, Chem. Eng. J. 334 (2018) 1055–1064.
[43] Y. Zhong, Q. Deng, Q. Yao, C. Lu, P. Zhang, H. Li, J. Wang, Z. Zeng, J. Zou, S. Deng, Functionalized biochar with superacidity and hydrophobicity as a highly efficient catalyst in the synthesis of renewable high-density fuels, ACS Sustain. Chem. Eng. 8 (2020) 7785–7794.
[44] C. Wang, D. Wu, H. Wang, Z. Gao, F. Xu, K. Jiang, A green and scalable route to yield porous carbon sheets from biomass for supercapacitors with high capacity, J. Mater. Chem. 6 (2018) 1244–1254.
[45] M. Zhang, M. Wu, Q. Liu, X. Wang, T. Lv, L. Jia, Graphene oxide mediated cellulose-derived carbon as a highly selective catalyst for the hydrolysis of cellulose to glucose, Appl. Catal. A-Gen. 545 (2017) 218–224.
[46] Y. Jin, C. Lai, Y. Li, X. Cheng, Preparation and catalytic performance of biomass-based solid acid catalyst from Pennisetum sinense for cellulose hydrolysis, Int. J. Biol. Macromol. 165 (2020) 1149–1155.
[47] H. Yang, Y. Yan, Y. Liu, F. Zhang, R. Zhang, Y. Meng, M. Li, S. Xie, B. Tu, D. Zhao, A simple melt impregnation method to synthesize ordered mesoporous carbon and carbon nanofiber bundles with graphitized structure from pitches, J. Phys. Chem. B 108 (2004) 17320–17328.
[48] M. Li, Q. Zhang, B. Luo, C. Chen, S. Wang, D. Min, Lignin-based carbon solid acid catalyst prepared for selectively converting fructose to 5-hydroxymethylfurfural, Ind. Crop. Prod. 145 (2020), 111920.
[49] X. Li, Y. Zuo, Y. Zhang, Y. Fu, Q. Guo, In situ preparation of K_2CO_3 supported kraft lignin activated carbon as solid base catalyst for biodiesel production, Fuel 113 (2013) 435–442.
[50] Y. Li, H. Liu, C. Song, X. Gu, H. Li, W. Zhu, S. Yin, C. Han, The dehydration of fructose to 5-hydroxymethylfurfural efficiently catalyzed by acidic ion-exchange resin in ionic liquid, Bioresour. Technol. 133 (2013) 347–353.
[51] S. Wang, L. Lyu, G. Sima, Y. Cui, B. Li, X. Zhang, L. Gan, Optimization of fructose dehydration to 5-hydroxymethylfurfural catalyzed by SO_3H-bearing lignin-derived ordered mesoporous carbon, Kor. J. Chem. Eng. 36 (2019) 1042–1050.
[52] M. Nahavandi, T. Kasanneni, Z. Yuan, C. Xu, S. Rohani, Efficient conversion of glucose into 5-hydroxymethylfurfural using a sulfonated carbon-based solid acid catalyst: an experimental and numerical study, ACS Sustain. Chem. Eng. 7 (2019) 11970–11984.
[53] K. Wang, C. Liang, Q. Zhang, F. Zhang, Synergistic catalysis of bronsted acid and lewis acid coexisted on ordered mesoporous resin for one-pot conversion of glucose to 5-hydroxymethylfurfural, ACS Omega 4 (2019) 1053–1059.
[54] Y. Wang, Z. Gu, W. Liu, Y. Yao, H. Wang, X. Xia, W. Li, Conversion of glucose into 5-hydroxymethylfurfural catalyzed by chromium(III) Schiff base complexes and acidic ionic liquids immobilized on mesoporous silica, RSC Adv 5 (2015) 60736–60744.
[55] A. Herbst, C. Janiak, Selective glucose conversion to 5-hydroxymethylfurfural (5-HMF) instead of levulinic acid with MIL-101Cr MOF-derivatives, New J. Chem. 40 (2016) 7958–7967.
[56] Y. Su, G. Chang, Z. Zhang, H. Xing, B. Su, Q. Yang, Q. Ren, Y. Yang, Z. Bao, Catalytic dehydration of glucose to 5-hydroxymethylfurfural with a bifunctional metal-organic framework, AIChE J. 62 (2016) 4403–4417.
[57] Y. Zhang, J. Zhao, K. Wang, L. Gao, M. Meng, Y. Yan, Green synthesis of acid-base bi-functional UiO-66-type metal-organic frameworks membranes supported on polyurethane foam for glucose conversion, ChemistrySelect 3 (2018) 9378–9387.
[58] Y. Wei, Y. Zhang, B. Li, C. Yan, Z. Da, M. Meng, C. Liu, Y. Yan, Fabrication of graphene oxide supported acid-base bifunctional metal-organic frameworks as efficient catalyst for glucose to 5-hydroxymethylfurfural conversion, Energy Technol 8 (2020), 1901111.
[59] Y. Zhang, B. Li, Y. Wei, C. Yan, M. Meng, Y. Yan, Direct synthesis of metal-organic frameworks catalysts with tunable acid-base strength for glucose dehydration to 5-hydroxymethylfurfural, J. Taiwan Inst. Chem. Eng. 96 (2019) 93–103.
[60] K. Li, M. Du, P. Ji, Multifunctional Tin-based heterogeneous catalyst for catalytic conversion of glucose to 5-hydroxymethylfurfural, ACS Sustain. Chem. Eng. 6 (2018) 5636–5644.
[61] L. Jiao, S. Sun, X. Meng, P. Ji, Sn-based porous coordination polymer synthesized with two ligands for tandem catalysis producing 5-hydroxymethylfurfural, Catalysts 9 (2019) 739.
[62] R. Liu, J. Chen, X. Huang, L. Chen, L. Ma, X. Li, Conversion of fructose into 5-hydroxymethylfurfural and alkyl levulinates catalyzed by sulfonic acid-functionalized carbon materials, Green Chem 15 (2013) 2895–2903.
[63] C.E. Bounoukta, C. Megias-Sayago, F. Ammari, S. Ivanova, A. Monzon, M.A. Centeno, J.A. Odriozola, Dehydration of glucose to 5-hydroxymethlyfurfural on bifunctional carbon catalysts, Appl. Catal. B Environ. 286 (2021), 119938.
[64] R.S. Thombal, V.H. Jadhav, Biomass derived β-cyclodextrin-SO_3H carbonaceous solid acid catalyst for catalytic conversion of carbohydrates to 5-hydroxymethylfurfural, Appl. Catal. A-Gen. 499 (2015) 213–216.
[65] A. Rusanen, R. Lahti, K. Lappalainen, J. Karkkainen, T. Hu, H. Romar, U. Lassi, Catalytic conversion of glucose to 5-hydroxymethylfurfural over biomass-based activated carbon catalyst, Catal. Today 357 (2020) 94–101.
[66] F. Guo, Z. Fang, T. Zhou, Conversion of fructose and glucose into 5-hydroxymethylfurfural with lignin-derived carbonaceous catalyst under microwave irradiation in dimethyl sulfoxide-ionic liquid mixtures, Bioresour. Technol. 112 (2012) 313–318.
[67] X. Fu, J. Dai, X. Guo, J. Tang, L. Zhu, C. Hu, Suppression of oligomer formation in glucose dehydration by CO_2 and tetrahydrofuran, Green Chem 19 (2017) 3334–3343.